Communication

# Structural Characterization of the Fleeting Ferric Peroxo Species in Myoglobin: Experiment and Theory

Masaki Unno, Hui Chen, Shusuke Kusama, Sason Shaik, and Masao Ikeda-Saito

*J. Am. Chem. Soc.*, **2007**, 129 (44), 13394-13395• DOI: 10.1021/ja076108x • Publication Date (Web): 12 October 2007



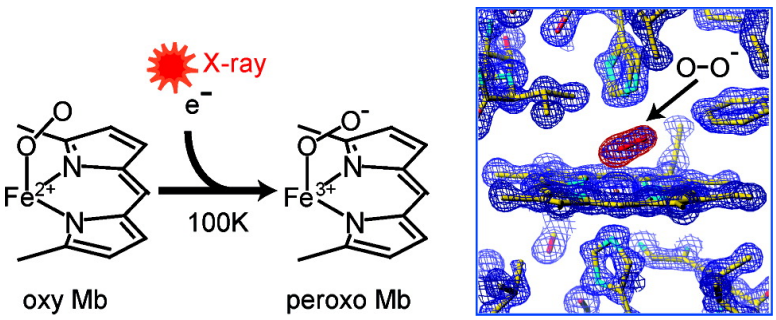


## More About This Article

Additional resources and features associated with this article are available within the HTML version:

- Supporting Information
- Links to the 5 articles that cite this article, as of the time of this article download
- Access to high resolution figures
- Links to articles and content related to this article
- Copyright permission to reproduce figures and/or text from this article

View the Full Text HTML

J|A|C|S
COMMUNICATIONS

Published on Web 10/12/2007

# Structural Characterization of the Fleeting Ferric Peroxo Species in Myoglobin: Experiment and Theory

Masaki Unno,*,†,‡ Hui Chen,§ Shusuke Kusama,† Sason Shaik,*,§ and Masao Ikeda-Saito*,†,‡

*Institute of Multidisciplinary Research for Advanced Materials, Tohoku University, Sendai 980-8577, Japan, RIKEN SPring-8 Center, Harima Institute, Sayo, Hyogo 679-5148, Japan, and Department of Organic Chemistry and the Lise Meitner-Minerva Center for Computational Quantum Chemistry, The Hebrew University of Jerusalem, Givat Ram Campus, 91904 Jerusalem, Israel*

Received August 14, 2007; E-mail: sason@yfaat.ch.huji.ac.il; mis2@tagen.tohoku.ac.jp

In catalytic cycles of mono-oxygenase heme enzymes, one-electron reduction of the ferrous oxy complex generates ferric peroxo ($Fe^{III}-OO^-$).[1] This process is often coupled with protonation of the distal peroxo oxygen through a distal pocket proton delivery system connected by a hydrogen bond to the ferrous oxy heme, resulting in formation of ferric hydroperoxo ($Fe^{III}-OOH$).[1,2] The second proton delivery to the hydroperoxo intermediate either yields an oxo ferryl porphyrin coupled with a porphyrin radical (compound I), a putative active form in P450 enzymes, or initiates hydroxylation of the heme *meso*-carbon in heme oxygenase (HO) without compound I formation.[1−3] Due to their very short life time and instability, characterization of peroxo and hydroperoxo intermediates of Mb, HO, P450, and peroxidase enzymes is proven difficult at ambient temperatures. This instability problem has been circumvented by radiolytic reduction of their respective ferrous oxy forms at cryogenic temperatures.[4] This method not only affords these unstable intermediates but also uncouples the reduction and protonation processes; that is, formations of ferric peroxo and hydroperoxo processes in some cases have been successfully attained. Proton delivery to the distal oxygen of the peroxo group depends on both temperature and the protein under study. For example, ferric peroxo Mb is stable near 100 K, and upon annealing >170 K, proton delivery takes place to yield ferric hydroperoxo Mb, while the peroxo group is readily protonated at substantially lower temperatures for HO (<6 K) and P450CAM (>55 K).[4,5] Despite these accumulating spectroscopic results, only crystal structures of hydroperoxo chloroperoxidase cryo-reduced by synchrotron radiation have been reported recently,[6] while that of ferric peroxo species has not been reported to date. We describe here the crystal structures of the ferrous oxy and ferric peroxo Mb, the latter of which has been generated by synchrotron radiation of the oxy form at 100 K. Optical absorption spectra of the crystals and hybrid QM/MM calculations have confirmed not only the formation of the peroxo species but also the integrities of the oxy and peroxo species during the diffraction data collection.

The crystal structure of the heme vicinity of the oxy Mb is shown in Figure 1 (left panel). Our initial attempt to collect diffraction data sets of oxy Mb by 1 Å synchrotron radiation at beamline NW12 of Photon Factory (Tsukuba, Japan) through a 0.6 mm aluminum attenuator for 1 s per 1° oscillation (total exposure time of 180 s) resulted in partial generation of ferric peroxo species as judged by the single-crystal absorption spectra.[7] We have successfully avoided this adverse problem caused by photoreduction due to the incident synchrotron beam by using 0.6 Å synchrotron radiation.[8] The shorter wavelength (higher energy) radiation has an advantage of lower absorption;[9] consequently, it can avoid generation of excess electrons. The optical absorption spectra of the oxy Mb crystal taken before and after the diffraction data collection affirm that the initial ferrous oxy state is well maintained during the diffraction data collection under the experimental conditions (Figure S1).[8] The oxy Mb structure refined to 1.25 Å resolution shows that the bound $O_2$ assumes a geometry summarized in Table 1, and that the imidazole side chain of His64 takes multiple conformation as reported in early high-resolution studies (PDB code 1A6M)[10] conducted using 1 Å synchrotron radiation. In the early work, spectroscopic examination of the crystal was not apparently conducted,[10] leaving some ambiguity in integrity of the ferrous oxy form. The apparent similar $Fe-O_2$ geometry (Table 1) might be regarded as an accidental coincidence because the structures of the ferrous oxy and ferric peroxo are virtually indistinguishable at the present level of resolutions as described below.

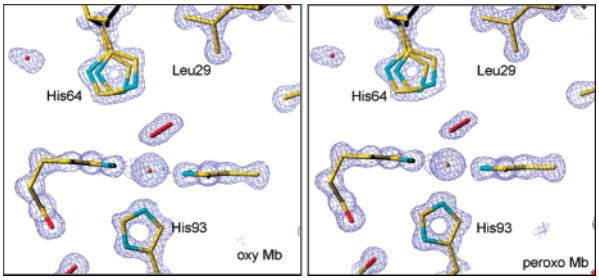


***Figure 1.*** Crystal structures of heme vicinity of oxy (left) and irradiated oxy (right) Mb; $2F_o-F_c$ electron density maps are at the $2\sigma$ level.

***Table 1.*** Fe Ligand Geometries in $P2_1$ Crystals of Sperm Whale Mb

| | distance (Å) | | | angle (°) |
|---|---|---|---|---|
| species | Fe–O | O–O | Fe–Prox···N$\epsilon$ | Fe–O–O |
| ferrous oxy | 1.83 | 1.25 | 2.08 | 124 |
| ferrous oxy[a] | 1.81 | 1.24 | 2.06 | 122 |
| ferric peroxo | 1.85 | 1.33 | 2.09 | 120 |

[a] From ref 10.

Irradiation with 1.0 Å synchrotron radiation for 1080 s at 100 K of the oxy crystal after the diffraction data collection converts the optical spectrum of the oxy form to the one very similar to the ferric peroxo species (Figure S1). Diffraction data collection of the irradiated crystal by 0.6 Å synchrotron radiation have not altered the optical absorption spectrum, indicating that the integrity of ferric peroxo appears to be maintained during the diffraction data collection. The crystal structure of the heme environment of the irradiated oxy Mb is shown in Figure 1 (right panel). The structure of the irradiated oxy form is similar to that of the ferrous oxy form including the axial ligand geometries (Table 1). Formation of

† Tohoku University.
‡ Harima Institute.
§ The Hebrew University of Jerusalem.


10.1021/ja076108x CCC: $37.00 

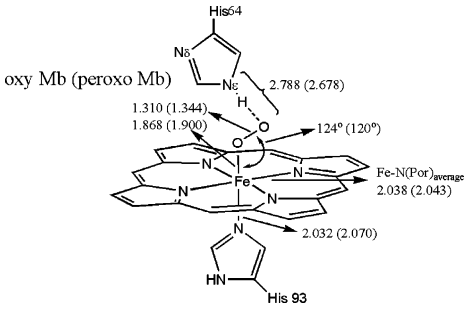


***Figure 2.*** The QM region in the QM/MM calculations for ground states of oxy and peroxo Mb (bond distances in angstroms and angles in degrees). The numbers for the peroxo Mb are in parentheses.

hydroperoxo Mb cannot take place at 100 K, and the O−O bond length observed in the crystal structure is shorter than that of ferric hydroperoxo of chloroperoxidase (1.5 Å).[6] These points strongly support the crystal structure of the irradiated oxy Mb as the peroxo Mb structure. However, because the visible region optical spectrum of the ferric peroxo species might not be able to readily discern from that of the ferric hydroperoxo form[7] and because the structure of the irradiated species is similar to that of the oxy form, theoretical studies have been conducted to ascertain the formation of ferric peroxo Mb.

Further support for the close geometric features of the oxy and peroxo Mb complexes is provided by the QM/MM calculations that were performed following common procedures used by the group in similar heme projects[11] and described in the Supporting Information (S5−S14). The active species of Mb was modeled with the QM system shown in Figure 2 along with the QM/MM optimized geometric parameters obtained with an all-electron basis set augmented with polarization and diffuse functions on iron and its immediate coordination shell (B2 on page S6). The optimized parameters agree reasonably well with the crystal structures and demonstrate that indeed the oxy and peroxo Mb complexes have very similar geometries (see more data in Table S2). The small differences between the two sets of data are expected, and a better convergence can be obtained using the theoretical values.[12] The existence of a strong hydrogen bonding interaction between N$\epsilon$H of His 64 and distal oxygen atom in both the oxy and the peroxo Mb was also confirmed by the QM/MM calculations. The positional disorder of His64 does not contradict the strong hydrogen bond since hydrogen bonds are not fixed structural elements and they exchange partners rather quickly even if strong.[13] In addition, QM/MM calculations of the HN$\delta$ form oxy Mb, proposed before to be possibly involved in the oxy Mb,[10] have revealed that this tautomer is 27.5 kcal/mol higher in energy than the HN$\epsilon$ form oxy Mb. This energy difference is completely dominated by the QM part of the QM/MM energy (Table S3), and as such, the involvement of the HN$\delta$ oxy Mb tautomer does not seem likely here.

The ground state of the peroxo Mb was calculated to be the doublet state, with a second lowest quartet state being 11.1 kcal/mol higher in energy at the QM/MM with a basis set that involves polarization and diffuse functions on all atoms in Figure 2 (see B3 on page S3). The unpaired electron of the doublet state resides in a $\pi^*_{OO}$ orbital, and this is apparent also from both the dismal spin density on iron (<0.2, Table S4) and the longish O−O bond distance (1.34 Å), which agrees well with crystal structure (1.33 Å). These features provide strong evidence for the X-ray assignment of the peroxo Mb. Further support is provided by the short hydrogen bond distance between N$\epsilon$H of His64 and distal oxygen atom (1.63 Å) in peroxo Mb, which is even shorter than that (1.77 Å) in oxy Mb. The ground state electronic structure of oxy Mb is an open-shell singlet in which the two unpaired $\alpha$ and $\beta$ electrons are mainly distributed on iron and the $O_2$ moiety;[14] a low lying triplet state is just 3.6 kcal/mol higher (excited states are described in Table S3).

In conclusion, the agreement between experiment and theory shows that the peroxo heme complex has been genuinely characterized in this work for the first time.

**Acknowledgment.** We thank H. Hori, T. Matsui, Y. Shiro, H. Sugimoto, T. Matsu, the members of Photon Factory, I. G. Denisov, and S. G. Sligar for their help and comments. Experiments at Photon Factory were conducted under the approval of 2005G255. M.I.-S. and M.U. are supported by Grants-in-Aid 18770080, 18370052, and 17GS0419 from JSPS and MEXT, Japan. S.S. is supported by an Israeli Science Foundation (ISF) grant.

**Supporting Information Available:** Experimental details, single crystal absorption spectra, computational details, QM/MM optimized structures, energies, spin and charge distributions, the orbital occupancy diagram of the studied electronic structures, singly occupied orbitals, and Cartesian coordinates of optimized oxy and peroxo Mb are found in Supporting Information. This material is available free of charge via the Internet at http://pubs.acs.org.

## References

(1) Sono, M.; Roach, M. P.; Coulter, E. D.; Dawson, J. H. *Chem. Rev.* **1996**, *96*, 2841−2887.
(2) (a) Denisov, I. G.; Makris, T. M.; Sligar, S. G.; Schlichting, I. *Chem. Rev.* **2005**, *105*, 2253−2277. (b) Unno, M.; Matsui, T.; Ikeda-Saito, M. *Nat. Prod. Rep.* **2007**, *24*, 553−570.
(3) (a) Harris, D. L.; Loew, G. H. *J. Am. Chem. Soc.* **1998**, *120*, 8941−8948. (b) Ogliaro, F.; de Visser, S. P.; Cohen, S.; Sharma, P. K.; Shaik, S. *J. Am. Chem. Soc.* **2002**, *124*, 2806−2817. (c) Kumar, D.; de Visser, S. P.; Shaik, S. *J. Am. Chem. Soc.* **2005**, *127*, 8204−8213. (d) Matsui, T.; Kim, S. H.; Jin, H.; Hoffman, B. M.; Ikeda-Saito, M. *J. Am. Chem. Soc.* **2006**, *128*, 1090−1091.
(4) (a) Kappl, R.; Höhn-Berlage, M.; Hüttermann, J.; Bartlett, N.; Symons, M. C. R. *Biochim. Biophys. Acta* **1985**, *827*, 327−343. (b) Davydov, R.; Makris, T. M.; Kofman, V.; Werst, D. W.; Sligar, S. G.; Hoffman, B. M. *J. Am. Chem. Soc.* **2001**, *123*, 1403−1415. (c) Davydov, R. M.; Yoshida, T.; Ikeda-Saito, M.; Hoffman, B. M. *J. Am. Chem. Soc.* **1999**, *121*, 10656−10657. (d) Denisov, I. G.; Makris, T. M.; Sligar, S. G. *J. Biol. Chem.* **2002**, *277*, 42706−42710.
(5) Davydov, R.; Chemerisov, S.; Werst, D. E.; Rajh, T.; Matsui, T.; Ikeda-Saito, M.; Hoffman, B. M. *J. Am. Chem. Soc.* **2004**, *126*, 15960−15961.
(6) Kühnel, K.; Derat, E.; Terner, J.; Shaik, S.; Schlichting, I. *Proc. Natl. Acad. Sci. U.S.A.* **2007**, *104*, 99−104.
(7) For the frozen solution absorption spectra of the ferrous oxy and ferric peroxo Mb, see: Ibrahim, M.; Denisov, I. G.; Makris, T. M.; Kincaid, J. R.; Sligar, S. G. *J. Am. Chem. Soc.* **2003**, *125*, 13714−13718.
(8) Monoclinic space group $P2_1$ sperm whale oxy Mb crystals were flash frozen at 100 K. Diffraction data were collected at BL44B2 of SPring-8 using 0.6 Å wavelength radiation with 10 s exposure for 1° oscillation. Total exposure time was 1800 s. Optical absorption spectra of the crystals before and after diffraction data collection were recorded by an on-line microspectrophotometer. Details for the crystallization, structural determination, diffraction data, and refinement statistics are found in the Supporting Information. Atomic coordinates and structural factors have been deposited to Protein Data Bank with accession codes of 2Z6S for oxy and 2Z6T for peroxo Mb.
(9) Schlichting, I.; Berendzen, J.; Chu, K.; Stock, A. M.; Maves, S. A.; Benson, D. E.; Sweet, R. M.; Ringe, D.; Petsko, G. A.; Sligar, S. G. *Science* **2000**, *287*, 1615−1622.
(10) Vojtechovský, J.; Chu, K.; Berendzen, J.; Sweet, R. M.; Schlichting, I. *Biophys. J.* **1999**, *77*, 2153−2174.
(11) (a) Schöneboom, J. C.; Lin, H.; Reuter, N.; Thiel, W.; Cohen, S.; Ogliaro, F.; Shaik, S. *J. Am. Chem. Soc.* **2002**, *124*, 8142−8151. (b) Derat, E.; Cohen, S.; Shaik, S.; Altun, A.; Thiel, W. *J. Am. Chem. Soc.* **2005**, *127*, 13611−13621.
(12) Ryde, U.; Nilsson, K. *J. Am. Chem. Soc.* **2003**, *125*, 14232−14233.
(13) Derat, E.; Shaik, S.; Rovira, C.; Vidossich, P.; Alfonso-Prieto, M. *J. Am. Chem. Soc.* **2007**, *129*, 6346−6347.
(14) For the oxyheme complex, DFT calculations underestimate the contribution of the Pauling bonding type and exaggerates the contribution of the $Fe^{III}O_2^{1-}$ (the Weiss configuration). See: Jensen, K. P.; Roos, B. O.; Ryde, U. *J. Inorg. Biochem.* **2005**, *99*, 978.

JA076108X